LANGMUIR Article
Cite This: Langmuir 2019, 35, 10625−10630
pubs.acs.org/Langmuir

Reversible Tuning between Isotropic and Anisotropic Sliding by One-Direction Mechanical Stretching on Microgrooved Slippery Surfaces

Yiyuan Zhang,[†,§] Yunlong Jiao,[*,†,§] Chao Chen,[†] Suwan Zhu,[†] Chuanzong Li,[‡] Jiawen Li,[†] Yanlei Hu,[†] Dong Wu,[*,†] and Jiaru Chu[†]

[†]CAS Key Laboratory of Mechanical Behavior and Design of Materials, Key Laboratory of Precision Scientific Instrumentation of Anhui Higher Education Institutes, Department of Precision Machinery and Precision Instrumentation, University of Science and Technology of China, Hefei 230026, China

[‡]School of Instrument Science and Opto-electronics Engineering, Hefei University of Technology, Hefei 230009, China

Supporting Information

ABSTRACT: Dynamically responsive liquid-infused interfacial materials have broad technological implications in manipulating droplet motions. However, present works are mainly about reversible tuning of the isotropic slippery surface; the reversible switching between isotropic and anisotropic sliding has not been deeply explored. Here, we report a kind of liquid-infused elastic-grooved surface (LIEGS) by femtosecond laser ablation and realize reversible switching between isotropic and anisotropic sliding by one-direction mechanical stretching. Under mechanical stretching and strain release, droplet motion can be reversibly switched between the sliding and pinned states along the perpendicular direction to the grooves, whereas the droplet keeps sliding along the parallel direction to the grooves. The mechanism of reversible switching mainly contributes to the decrease of film thickness during the stretching process in which the film thickness decreases from 13 to 4 μm with the increase of the strain from 0 to 60%. Finally, we demonstrate the real-time flexible control over a droplet sliding/pinned on the strain-changing LIEGS.

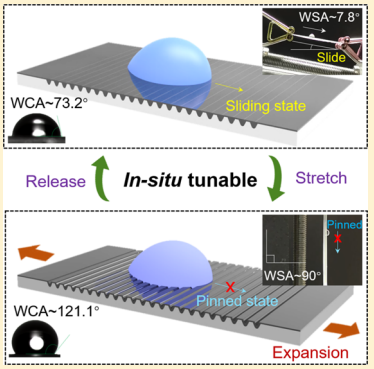

INTRODUCTION

Inspired by the peristome of *Nepenthes* pitcher plants, slippery liquid-infused porous surfaces (SLIPS) have been studied for several years. Aizenberg and co-workers first introduced the concept of liquid-infused surfaces, which consist of a lubricating liquid film locked in place by a porous substrate and have several excellent properties including self-cleaning, self-healing, anti-ice, anti-frost, anti-biofouling, exceptional liquid repellency, pressure stability, and so on.[1−6] Thus, a slippery surface has widespread applications in the fields of anti-frost,[3] drag reduction,[7] enhanced condensation,[8] and the smart dynamic control of a droplet.[9−24] For instance, the *Nepenthes* pitcher plants utilize the surface structure to lock in slippery liquid to hunt insects which step on them and slide from the rim to the bottom.[11] Yong et al. fabricated a slippery liquid-infused porous surface by femtosecond laser direct writing for promoting/inhibiting the growth of C6 glioma cells.[12,13] In addition, a large number of research studies have attempted to reveal the mechanism of controlling the liquid droplet on SLIPS. In general, SLIPS have better repellency to low surface tension liquids including all kinds of alkanes and so on, but the infused slippery liquid which completely covers the substrate multiscale micro-/nanostructure hinders the flexible control over liquid droplet dynamics.

Taking hints from dynamically responsive materials in nature, researchers have focused their study on dynamically adaptive SLIPS, which are capable of accessing a range of continuous and adjustable topographies to realize multifunctional surface properties. For example, Heng et al. prepared a kind of porous and conductive film to achieve electrically driven droplet motion by voltage and explored the effect of lubricant viscosity on self-healing properties.[14] They also fabricated a kind of photoelectric synergetic responsive SLIPS based on tailored anisotropic films generated by interfacial directional freezing.[15] Moreover, Hu et al. prepared a dynamically actuated liquid infused poroelastic film with control over droplet dynamics, which is achieved by voltage.[16] However, the above responsive strategies need complicated external energy inputs such as the extra electric energy when the voltage is applied to photoelectric synergetic responsive materials,[14−16] which may not be convenient for the manipulation of biological droplets.

Mechanical stretching is an environment-friendly, cost-effective method to tune the surface wettability. Kim and co-workers fabricated an elastic composite substrate using photolithography to achieve switchable wettability between the lotus effect and the petal effect with mechanical strain.[19] Yin et al. also prepared a kind of hierarchical wrinkles on the

Received: April 8, 2019
Revised: May 28, 2019
Published: July 10, 2019

DOI: 10.1021/acs.langmuir.9b01035
Langmuir 2019, 35, 10625−10630

plasma desorption mass spectrometry to realize a potential multifunctional smart window and structural color.[25] However, the above tunable process is not based on slippery surfaces; thus, these surfaces are only suitable for water droplet and not for diverse droplets. Yao et al. designed a kind of adaptive liquid-infused porous film by chemical adhesive to realize tunable transparency and wettability by mechanical stretching,[26] which can be used for manipulating various liquids, for example octane, decane, and so on. However, it is worth noting that the fabrication of the elastic materials in the above research studies not only is a multistep process and time-consuming but also easily causes potential environmental pollution by chemical agents during the tuning process. Most importantly, present works are mainly concentrated on the reversible tuning of isotropic elastic materials;[16,26] the reversible switching between isotropic and anisotropic sliding by mechanical stretching on the liquid-infused elastic surface has not been deeply researched. Moreover, to achieve progressive practical applications, the influence of spin-coating speed, droplet volume, and laser power on the degree of sliding angles at different strains and the mechanism of droplet interaction with micro-grooved slippery surfaces should be further systemically studied.

Herein, we report a kind of one-dimensional microgroove slippery surface by femtosecond laser scanning and liquid infusion, which can realize reversible switching between isotropic and anisotropic sliding by one-direction mechanical stretching. Through mechanical stretching and strain release, droplet motion is reversibly switched between the sliding and pinned states along the perpendicular direction to the grooves, whereas the droplet is always sliding along the parallel direction to the grooves. The mechanism of reversible switching mainly contributes to the decrease of the lubricant film thickness during the stretching process, and the droplet contacts with the uneven oil film at high strain, which shows a high hysteresis resistance to the liquid. Additionally, the relationship between the sliding angle and the strain under different rotation speeds, droplet volumes, and laser power is explored. Finally, we demonstrate the real-time flexible control of droplet sliding/pinned on the strain-changing liquid-infused elastic grooved surface (LIEGS). We believe that this work will provide new insights to researchers in achieving the mechanical responsive in situ tunable droplet motion on the smart responsive liquid-infused surface for broad applications.

RESULT AND DISCUSSION

Figure 1a shows the fabrication process of LIEGS. First, the grooved structure on a silicone sheet is prepared by femtosecond laser ablation in the homemade optical fabrication system, which has been introduced in our previous research studies.[27−29] It is worth noting that femtosecond laser is a facile strategy to process superwetting microstructures in the fabrication of the slippery surface, which has been deeply explored in many research studies.[30−33] Then, the silicone oil is added on the textured surface by spin-coating to form a stable and uniform lubricant film so that the LIEGS is prepared. It is demonstrated in Figure 1b that the droplet motion state is affected by different tensile strains. Along the perpendicular direction to the grooves, the water droplet can easily slide on the original LIEGS, whereas it is pinned when the LIEGS is stretched to a certain degree. As shown in Figure 1c, there is a micro-scale grooved structure and nano-scale particles which are in favor of forming a superhydrophobic substrate so as to

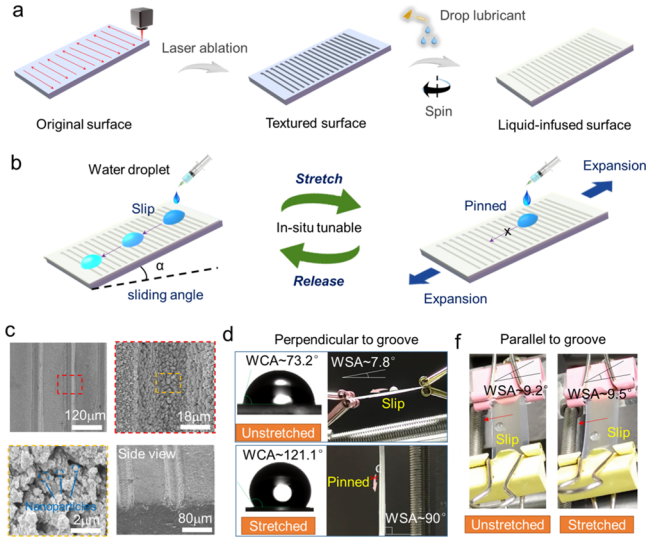

Figure 1. Fabrication process, surface characterization, and application of the mechanical responsive LIEGS. (a) Detailed fabrication process of LIEGS including two main steps: laser ablation and lubrication process. (b) Schematics showing the in situ tuning from sliding to pinned, which is dependent on the applied tensile strain. (c) Scanning electron microscopy of the silicone sheet patterned with an array of grooves. The grooves have an approximately V-shaped cross section which can store the lubricant silicone oil. Because of the intrinsic hydrophobic property of the silicone sheet, the LIEGS presents the superhydrophobicity. (d) Along the perpendicular direction to the grooves, the unstretched LIEGS demonstrates a smaller WCA (∼73.2°) than the stretched one (∼121.1°) because of the reduced oil film thickness and the droplet will pin on the stretched LIEGS with a WSA (∼90°) while easily sliding on the unstretched one (∼7.8°). (e) Along the parallel direction to the grooves, the droplet will slide easily (∼8.5°) on both the stretched and unstretched states of LIEGS.

hold a stable and uniform lubricant film. Figure 1d shows water contact angle (WCA) and water sliding angle (WSA) on the unstretched and stretched LIEGS along the perpendicular direction to the grooves. It can be seen that the WCA (∼73.2°) on the unstretched LIEGS is smaller than that (∼121.1°) on the stretched LIEGS because of the exposed hydrophobic silicone sheet substrate and the enhancement of wettability by textured structures. Additionally, the water droplet could easily slide on the unstretched LIEGS with a WSA of ∼7.8°, whereas it is pinned on the stretched LIEGS even as the tilted angle comes to ∼90°. Figure 1e demonstrates the sliding behavior of the droplet along the parallel direction to the grooves. It can be seen that the droplet slides on both stretched and unstretched LIEGS with a smaller WSA of ∼9°. Therefore, we have realized reversible switching between isotropic and anisotropic sliding on the LIEGS by one-direction mechanical stretching.

In order to explain the mechanism of dynamic control over droplet motions on the LIEGS, we study the force analysis of the droplet on the stretched LIEGS. As shown in Figure 2a, the driving force of droplet motion is the axis-direction component of gravity, which is calculated as $F_{driven} = \rho \times V \times g \times \sin \alpha$ (ρ, V, g, and α denote the water density, water volume, gravitational acceleration, and tilted angle of the substrate). The adhesive force and another component of the gravity guarantee the droplet's interaction with the LIEGS. The dominating motion resistance is caused by the contact angle

DOI: 10.1021/acs.langmuir.9b01035
Langmuir 2019, 35, 10625−10630

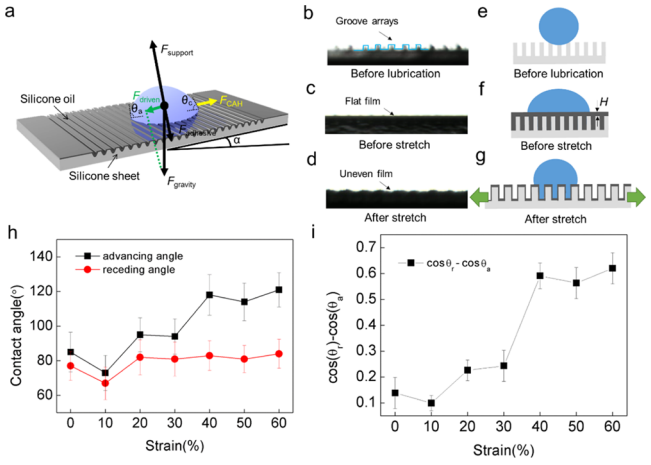

Figure 2. Force analysis and mechanism of dynamic control over droplet motions. (a) Schematics showing the force analysis of the droplet deposited on the LIEGS. (b–d) Optical images of LIEGS side profiles before lubrication, before stretching, and after stretching. (e–g) Three types of droplet wetting state by changing the silicone oil thickness. (h) Relationship between advancing/receding contact angle and the tensile strain. (i) Relationship between the equation cos θ_R − cos θ_A and the tensile strain.

hysteresis (CAH) of the droplet. The CAH resistance can be calculated as the equation $F_{CAH} = \gamma \times L \times (\cos \theta_R - \cos \theta_A)$,[34] where γ, L, θ_A, and θ_R represent the surface tension of water (~72 mN/m), droplet's characteristic length, and the advancing and receding contact angle of the water droplet. It is worth noting that the CAH resistance F_{CAH} mainly determines whether or not the droplet can slide on LIEGS, which is closely related to the thickness of the oil film (Figure 2b–g). When the lubricant oil is not applied to the structure, the profile of the grooves is easily visible (Figure 2b) and the droplet is in a superhydrophobic state (Figure 2e). After infusing the silicone oil into the groove, the water droplet contacts the flat silicone oil film (Figure 2c) on the unstretched LIEGS and the sample shows a low CAH with a smaller WCA (Figure 2f). The oil film thickness (H) is the distance between the upper side of the film and the top of the grooves. If we apply a strain by stretching the LIEGS, the lubricant liquid will sink into the grooved structure[13] and the oil film becomes thin and uneven (Figure 2d), so that the droplet shows a high CAH on the uneven film with a bigger WCA (Figure 2g). Moreover, we study the quantitative relationship between the advancing/receding angle and the strain. As the strain increases from 0 to 60%, the advancing contact angle increases from 85° to 121° whereas the receding contact angle stays almost the same (Figure 2h). Furthermore, we calculated the equation cos θ_R − cos θ_A, which corresponds to the resistance of F_{CAH} according to the equation of CAH resistance,[34] and the results indicate that F_{CAH} increases with the increase of strain (Figure 2i) so that the droplet motion could be tuned by stretching the LIEGS.

We also conduct a series of oil thickness measurements and water droplet sliding experiments on the LIEGS with different experimental parameters, such as spin-coating speed, droplet volume, and laser power (Figure 3). It is apparent in Figure 3a that the silicone oil thickness decreases gradually from 13 to 4 μm with the increase of the strain from 0 to 60% when the LIEGS is stretched, which contributes to the variation of the droplet CAH resistance. Then, we studied the relationship

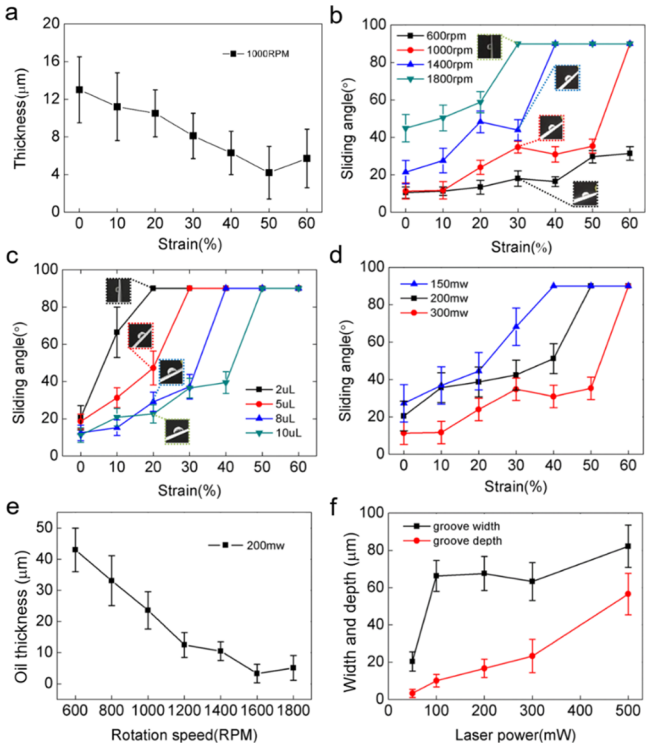

Figure 3. Measurements of oil thickness and sliding angles for different parameters including strain, spin-coating rotation speed, test droplet volume, and laser power, and the groove width and depth analysis under different laser power. (a) Relationship between the silicone oil thickness and the tensile strain. (b–d) Influence of spin-coating rotation speed, test droplet volume, and laser power on the relationship between the sliding angle and the tensile strain. (e) Measurements of oil film thickness for different spin-coating rotation speeds. (f) Influence of laser power on the groove width and depth.

between the WSA and the strain under different parameters (Figure 3b–d). Figure 3b shows the effect of rotation speed on the WSA at different strains. It can be seen that under the same strain the WSA increases with the increase of the rotation speed, which is mainly caused by the variation of the oil thickness. In general, the rotation speed directly determines the lubricant thickness. As the rotation speed increases, the oil thickness would decrease (Figure 3e) so that the droplet contacts with the uneven oil film caused by the grooved structure and shows a high CAH and sliding angle. Additionally, the WSA is influenced by the droplet volume. It can be seen that an 8 μL droplet can easily slide with a sliding angle of ~23° whereas the sliding angle increases to ~90° for a 2 μL droplet because of the smaller component of gravity (Figure 3c). Besides, laser power can affect the droplet sliding angle by changing the width and depth of the grooves. When the laser power increases from 150 to 300 mW, the consequent depth of the grooved structure increases from 20 to 82 μm, which can store more lubricant oil so that the droplet can slide easily under the same strain (Figure 3d,f).

On the basis of the above experiment results, mechanical responsive capture/release of droplets can be achieved (Figure 4 and Movie S1). As a proof-of-concept, a 5 μL water drop was deposited on the LIEGS in the case of zero tensile strain, and its sliding behavior was recorded as the LIEGS was stretched to different degrees. Figure 4a shows that a water drop that was deposited on the LIEGS with a tilted angle of ~17°. The droplet easily slides once it touches the surface because the

DOI: 10.1021/acs.langmuir.9b01035
Langmuir 2019, 35, 10625−10630

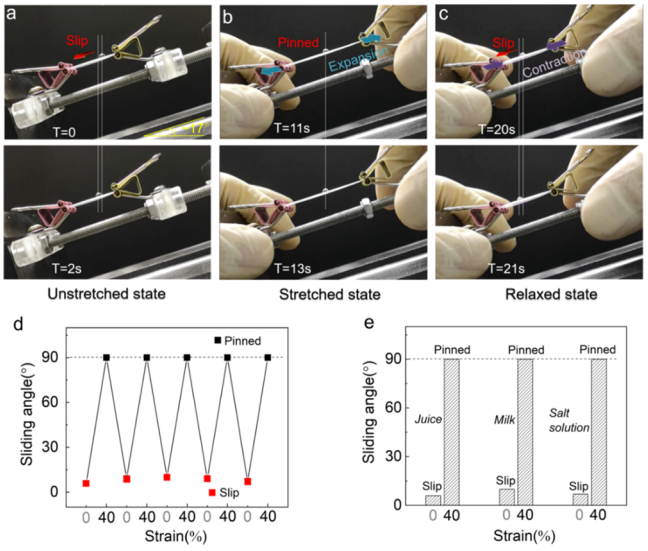

Figure 4. Demonstration of mechanical responsive in situ dynamic control of droplet motions on the LIEGS given a tilted angle of 17°. (a) When the LIEGS is not stretched, the droplet has a sliding angle which is smaller than the tilted angle so that it can easily slide on the LIEGS. (b) When the tensile strain is applied onto the LIEGS, the sliding angle of the droplet enlarges too much so that the droplet is pinned on the surface. (c) When the strain is released, the sliding angle recovers as before, which is smaller than the tilted angle so that the droplet slides off again. (d) Reversible tests for the switching between pinned state and sliding states. (e) Three types of liquid droplet tests for the relationship between the sliding angle and the tensile strain.

sliding angle was smaller than the tilted angle. When the strain was applied to the LIEGS, the water droplet slowed and stopped in a very short time because the droplet assumed a higher sliding angle state, and sliding angle was larger than the tilted angle. When there was a continual strain on the LIEGS, the droplet was pinned on it (Figure 4b). When the strain was removed, the droplet was released and slid off again on the surface because of the regressive sliding angle (Figure 4c). On the basis of the above results, mechanical responsive control of water droplet sliding on LIEGS was achieved by alternating the stretching strain. Moreover, the different states including pinned and sliding could be reversibly switched a large number of times by applying different tensile strains (Figure 4d). The LIEGS has been proved to own the dynamic in situ tuning property for different types of liquid including juice, milk, and salt solution (Figure 4e).

CONCLUSIONS

In conclusion, we fabricate a kind of grooved liquid-infused silicone sheet surface to achieve reversible switching between isotropic and anisotropic sliding by one-direction mechanical stretching. Through the mechanical stretching and releasing of the LIEGS, droplet motion is reversible switching between the sliding and pinned states along the perpendicular direction to the grooves, whereas the droplet keeps sliding along the parallel direction to the grooves. The mechanism of reversible switching mainly contributes to the decrease of the lubricant film thickness during the stretching process, and the droplet contacts with the uneven oil film which shows a high hysteresis resistance to the liquid. It is worth noting that the oil thickness is influenced by many experimental parameters, such as rotation speed and laser power. On the basis of the above manipulation strategy, mechanical responsive capture/release of droplets can be achieved. We have realized the real-time flexible control of droplet sliding/pinned on the strain-changing LIEGS, which could be reversibly switched a large number of times with great fatigue stability and it is also suitable for different kinds of liquids, such as milk, juice, and salt solution. This work may provide a new strategy to fabricate adaptive and dynamic SLIPS for broad potential applications.

EXPERIMENTAL DETAILS

Materials. Silicone sheets (200 μm thick) were purchased from Chun Shi New Material Tech. Co., Ltd., Nanjing, China. The lubricant silicone oil was used for the preparation of the LIEGS, and the LIEGS was obtained by spin-coating the prepared silicone oil at a certain speed (ranged from 600 to 1800 rpm) for 3 min. The distilled water was served as contact angle measurement materials.

Femtosecond Laser Fabrication. The grooved structure on the sample was achieved by line-by-line laser ablation. The laser beam (104 fs, 1 kHz, central wavelength 800 nm) from a regenerative amplified Ti:Sapphire femtosecond laser system (Solstice Ace, Spectra Physics, USA) was employed for processing. The laser beam was guided onto the silicone sheet by a scanning galvanometer (Sunny Technology, China), which was equipped with a 100 mm telecentric $f\theta$ lens to make the beam focus and scan along the x/y coordinate direction. The scanning period between two adjacent lines is 150 μm, the laser processed area is 8 × 15 mm, and scanning speed is 4 mm/s. The laser power ranges from 150 to 300 mW.

Characterization. The micro/nanostructure ablated by laser was characterized by using a tungsten filament scanning electron microscope (JSM-6700F, Japan). The contact angles of the water droplet (ranged from 2 to 10 μL) in air were measured using a CA100C contact-angle system (Innuo, China) with the sessile drop method. The average values were obtained by measuring three drops at different locations on the same sample. All the contact angle measurements were conducted at 10% humidity and 20 °C temperature.

In Situ Manipulation of Liquid Motions on the LIEGS. The as-prepared samples were put on the tilted platform. We use the microliter injector to add different liquids (water, juice, and milk) on the LIEGS. A home-made film stretcher was used to add different strains to the LIEGS, which results in the slipping/pinned under the unstretched/stretched state, respectively. The detailed tuning process of droplet motion was recorded by a digital camera.

ASSOCIATED CONTENT

Supporting Information

The Supporting Information is available free of charge on the ACS Publications website at DOI: 10.1021/acs.langmuir.9b01035.

Mechanical responsive in situ dynamic control of droplet motions on the LIEGS (AVI)

AUTHOR INFORMATION

Corresponding Authors

*E-mail: jyljjw@ustc.edu.cn (Y.J.).
*E-mail: dongwu@ustc.edu.cn (D.W.).

ORCID

Yunlong Jiao: 0000-0001-7718-7342
Jiawen Li: 0000-0003-3950-6212
Yanlei Hu: 0000-0003-1964-0043
Dong Wu: 0000-0003-0623-1515
Jiaru Chu: 0000-0001-6472-8103

DOI: 10.1021/acs.langmuir.9b01035
Langmuir 2019, 35, 10625−10630

Author Contributions

[§]Y.Z.and Y.J. contributed equally to this work.

Notes

The authors declare no competing financial interest.

■ ACKNOWLEDGMENTS

This work was supported by the National Natural Science Foundation of China (nos. 51805508, 51875544, and 61805230), the Fundamental Research Funds for the Central Universities (nos. WK2090090025, WK2090090024), the China Postdoctoral Science Foundation (no. 2018M642534), the National Key R&D Program of China (2017YFB1104303), the Chinese Academy of Sciences Instrument Project (YZ201566). Y.Z.and Y.J. contribute equally to this work. We acknowledge the Experimental Center of Engineering and Material Sciences at USTC for the fabrication and measuring of samples.

■ REFERENCES

(1) Wong, T.-S.; Kang, S. H.; Tang, S. K. Y.; Smythe, E. J.; Hatton, B. D.; Grinthal, A.; Aizenberg, J. Bioinspired self-repairing slippery surfaces with pressure-stable omniphobicity. *Nature* **2011**, *477*, 443.

(2) Wang, S.; Liu, K.; Yao, X.; Jiang, L. Bioinspired surfaces with superwettability: new insight on theory, design, and applications. *Chem. Rev.* **2015**, *115*, 8230−8293.

(3) Kim, P.; Wong, T.-S.; Alvarenga, J.; Kreder, M. J.; Adorno-Martinez, W. E.; Aizenberg, J. Liquid-infused nanostructured surfaces with extreme anti-ice and anti-frost performance. *ACS Nano* **2012**, *6*, 6569−6577.

(4) Epstein, A. K.; Wong, T.-S.; Belisle, R. A.; Boggs, E. M.; Aizenberg, J. Liquid-infused structured surfaces with exceptional anti-biofouling performance. *Proc. Natl. Acad. Sci. U.S.A.* **2012**, *109*, 13182−13187.

(5) Smith, J. D.; Dhiman, R.; Anand, S.; Reza-Garduno, E.; Cohen, R. E.; McKinley, G. H.; Varanasi, K. K. Droplet mobility on lubricant-impregnated surfaces. *Soft Matter* **2013**, *9*, 1772−1780.

(6) Yao, L.; He, J. Recent progress in antireflection and self-cleaning technology-From surface engineering to functional surfaces. *Prog. Mater. Sci.* **2014**, *61*, 94−143.

(7) Rosenberg, B. J.; Van Buren, T.; Fu, M. K.; Smits, A. J. Turbulent drag reduction over air-and liquid-impregnated surfaces. *Phys. Fluids* **2016**, *28*, 015103.

(8) Anand, S.; Paxson, A. T.; Dhiman, R.; Smith, J. D.; Varanasi, K. K. Enhanced condensation on lubricant-impregnated nanotextured surfaces. *ACS Nano* **2012**, *6*, 10122−10129.

(9) Manna, U.; Lynn, D. M. Fabrication of liquid-infused surfaces using reactive polymer multilayers: principles for manipulating the behaviors and mobilities of aqueous fluids on slippery liquid interfaces. *Adv. Mater.* **2015**, *27*, 3007−3012.

(10) Boreyko, J. B.; Polizos, G.; Datskos, P. G.; Sarles, S. A.; Collier, C. P. Air-stable droplet interface bilayers on oil-infused surfaces. *Proc. Natl. Acad. Sci. U.S.A.* **2014**, *111*, 7588−7593.

(11) Bohn, H. F.; Federle, W. Insect aquaplaning: Nepenthes pitcher plants capture prey with the peristome, a fully wettable water-lubricated anisotropic surface. *Proc. Natl. Acad. Sci. U.S.A.* **2004**, *101*, 14138−14143.

(12) Yong, J.; Chen, F.; Yang, Q.; Fang, Y.; Huo, J.; Zhang, J.; Hou, X. Nepenthes inspired design of self-repairing omniphobic slippery liquid infused porous surface (SLIPS) by femtosecond laser direct writing. *Adv. Mater. Interfaces* **2017**, *4*, 1700552.

(13) Yong, J.; Huo, J.; Yang, Q.; Chen, F.; Fang, Y.; Wu, X.; Liu, L.; Lu, X.; Zhang, J.; Hou, X. Femtosecond Laser Direct Writing of Porous Network Microstructures for Fabricating Super-Slippery Surfaces with Excellent Liquid Repellence and Anti-Cell Proliferation. *Adv. Mater. Interfaces* **2018**, *5*, 1701479.

(14) Wang, Z.; Heng, L.; Jiang, L. Effect of lubricant viscosity on the self-healing properties and electrically driven sliding of droplets on anisotropic slippery surfaces. *J. Mater. Chem. A* **2018**, *6*, 3414−3421.

(15) Wang, Z.; Liu, Y.; Guo, P.; Heng, L.; Jiang, L. Photoelectric synergetic responsive slippery surfaces based on tailored anisotropic films generated by interfacial directional freezing. *Adv. Funct. Mater.* **2018**, *28*, 1801310.

(16) Oh, I.; Keplinger, C.; Cui, J.; Chen, J.; Whitesides, G. M.; Aizenberg, J.; Hu, Y. Dynamically actuated liquid-infused poroelastic film with precise control over droplet dynamics. *Adv. Funct. Mater.* **2018**, *28*, 1802632.

(17) Hao, C.; Li, J.; Liu, Y.; Zhou, X.; Liu, Y.; Liu, R.; Che, L.; Zhou, W.; Sun, D.; Li, L.; Xu, L. Superhydrophobic-like tunable droplet bouncing on slippery liquid interfaces. *Nat. Commun.* **2015**, *6*, 7986.

(18) Luo, J. T.; Geraldi, N. R.; Guan, J. H.; McHale, G.; Wells, G. G.; Fu, Y. Q. Slippery liquid-infused porous surfaces and droplet transportation by surface acoustic waves. *Phys. Rev. Appl.* **2017**, *7*, 014017.

(19) Park, J. K.; Yang, Z.; Kim, S. Black Silicon/Elastomer Composite Surface with Switchable Wettability and Adhesion between Lotus and Rose Petal Effects by Mechanical Strain. *ACS Appl. Mater. Interfaces* **2017**, *9*, 33333−33340.

(20) Kamei, J.; Yabu, H. On-demand liquid transportation using bioinspired omniphobic lubricated surfaces based on self-organized honeycomb and pincushion films. *Adv. Funct. Mater.* **2015**, *25*, 4195−4201.

(21) Khalil, K. S.; Mahmoudi, S. R.; Abu-Dheir, N.; Varanasi, K. K. Active surfaces Ferrofluid-impregnated surfaces for active manipulation of droplets. *Appl. Phys. Lett.* **2014**, *105*, 041604.

(22) Urata, C.; Masheder, B.; Cheng, D. F.; Hozumi, A. Unusual dynamic dewetting behavior of smooth perfluorinated hybrid films: potential advantages over conventional textured and liquid-infused perfluorinated surfaces. *Langmuir* **2013**, *29*, 12472−12482.

(23) Lee, C.; Kim, H.; Nam, Y. Drop impact dynamics on oil-infused nanostructured surfaces. *Langmuir* **2014**, *30*, 8400−8407.

(24) Dai, X.; Sun, N.; Nielsen, S. O.; Stogin, B. B.; Wang, J.; Yang, S.; Wong, T.-S. Hydrophilic directional slippery rough surfaces for water harvesting. *Sci. Adv.* **2018**, *4*, No. eaaq0919.

(25) Lin, G.; Chandrasekaran, P.; Lv, C.; Zhang, Q.; Tang, Y.; Han, L.; Yin, J. Self-similar hierarchical wrinkles as a potential multifunctional smart window with simultaneously tunable transparency, structural color, and droplet transport. *ACS Appl. Mater. Interfaces* **2017**, *9*, 26510−26517.

(26) Yao, X.; Hu, Y.; Grinthal, A.; Wong, T.-S.; Mahadevan, L.; Aizenberg, J. Adaptive fluid-infused porous films with tunable transparency and wettability. *Nat. Mater.* **2013**, *12*, 529.

(27) Jiao, Y.; Lv, X.; Zhang, Y.; Li, C.; Li, J.; Wu, H.; Xiao, Y.; Wu, S.; Hu, Y.; Wu, D.; Chu, J. Pitcher plant-bioinspired bubble slippery surface fabricated by femtosecond laser for buoyancy-driven bubble self-transport and efficient gas capture. *Nanoscale* **2019**, *11*, 1370−1378.

(28) Jiao, Y.; Li, C.; Wu, S.; Hu, Y.; Li, J.; Yang, L.; Wu, D.; Chu, J. Switchable underwater bubble wettability on laser-induced titanium multiscale micro-/nanostructures by vertically crossed scanning. *ACS Appl. Mater. Interfaces* **2018**, *10*, 16867.

(29) Jiao, Y.; Li, C.; Lv, X.; Zhang, Y.; Wu, S.; Chen, C.; Hu, Y.; Li, J.; Wu, D.; Chu, J. In situ tunable bubble wettability with fast response induced by solution surface tension. *J. Mater. Chem. A* **2018**, *6*, 20878−20886.

(30) Yong, J.; Chen, F.; Li, M.; Yang, Q.; Fang, Y.; Huo, J.; Hou, X. Remarkably simple achievement of superhydrophobicity, superhydrophilicity, underwater superoleophobicity, underwater superoleophilicity, underwater superaerophobicity, and underwater superaerophilicity on femtosecond laser ablated PDMS surfaces. *J. Mater. Chem. A* **2017**, *5*, 25249−25257.

(31) Zhang, J.; Yong, J.; Yang, Q.; Chen, F.; Hou, X. Femtosecond Laser-Induced Underwater Superoleophobic Surfaces with Reversible pH-Responsive Wettability. *Langmuir* **2019**, *35*, 3295.

DOI: 10.1021/acs.langmuir.9b01035
Langmuir 2019, 35, 10625−10630

(32) Yong, J.; Singh, S. C.; Zhan, Z.; Chen, F.; Guo, C. How To Obtain Six Different Superwettabilities on a Same Microstructured Pattern: Relationship between Various Superwettabilities in Different Solid/Liquid/Gas Systems. *Langmuir* **2019**, *35*, 921−927.
(33) Yong, J.; Singh, S. C.; Zhan, Z.; Huo, J.; Chen, F.; Guo, C. Reducing Adhesion for Dispensing Tiny Water/Oil Droplets and Gas Bubbles by Femtosecond Laser-Treated Needle Nozzles: Superhydrophobicity, Superoleophobicity, and Superaerophobicity. *ChemNanoMat* **2019**, *5*, 241−249.
(34) Yu, C.; Zhu, X.; Li, K.; Cao, M.; Jiang, L. Manipulating bubbles in aqueous environment via a lubricant-infused slippery surface. *Adv. Funct. Mater.* **2017**, *27*, 1701605.

DOI: 10.1021/acs.langmuir.9b01035
Langmuir 2019, 35, 10625−10630